

Creep and Stress Relaxation Performance of Rubber Matrix Sealing Composites after Fatigue Loading

Xiaoming Yu¹, Bin Zhang^{1*}, and Boqin Gu²

¹*School of Mechanical Engineering, Changshu Institute of Technology, Changshu 215500, China*

²*School of Mechanical and Power Engineering, Nanjing Tech University, Nanjing 211816, China*

(Received February 27, 2021; Revised May 14, 2021; Accepted May 26, 2021)

Abstract: The most common working condition in the static seal connection system is load fluctuation. The failure mechanism of sealing material caused by load fluctuation is more complicated than that under static load. This work develops an experimental method to research mechanical property of short fiber reinforced rubber matrix sealing composites (SFRC). The damage behavior of creep and stress relaxation after different fatigue cycles is obtained. The microscopic defects are observed and analyzed by scanning electron microscope (SEM). The effects of different fatigue cycles on the damage of materials are found, and the damage modes of SFRC are determined. Based on macroscopic phenomena and microscopic mechanism, the parameters of new creep and stress relaxation models of SFRC after different fatigue cycles are determined, respectively. It can be found that the phenomenological model can well characterize fatigue behavior of SFRC.

Keywords: Fiber reinforced composite, Rubber, Fatigue, Creep, Stress relaxation

Introduction

Short fiber reinforced rubber matrix sealing composites (SFRC) is a new kind of structural material. Large specific stiffness, high specific strength and designable performance are the greatest advantages of it. As one of main bearing parts, it has been used in electronics and electrical, nuclear and automobile industries extensively [1,2]. The higher requirements for the safety and reliability of the sealing structure pose a challenge with the development of modern industry. The seal failure not only causes energy and raw materials waste, but also generates equipment abandonment, shutdown, loss of life and personal injury, and serious environmental pollution. Therefore, the performance evaluation of new sealing composite with creep, stress relaxation, compress resilience ratio and good medium adaptability is the key to high parameter sealing [3,4].

The most common working condition in the static seal connection system is load fluctuation. The failure mechanism of sealing material occurred by load fluctuation is more complicated than that by static load. At present, the research on the mechanical properties of composites is mainly focused on the compression, tensile and torsion properties under static load, while the research on mechanical properties under dynamic load is rarely seen [5-7]. El Sawi *et al.* [8]. investigated the initiation and evolution of failure of flax fiber reinforced resin matrix composites under fatigue load. The crack propagation of materials at different damage stages was observed. It can be found that the initiation and evolution of cracks were mostly occurred by interfacial debonding. Garcea *et al.* [9]. investigated the initiation and expansion failure process of polymer composites under fatigue load. The microcosmic failure modes of

composites at different fatigue stages were obtained by testing methods. It can be found that the damage mode of interfacial debonding had an important influence on the fatigue behavior of composites.

Creep and stress relaxation are well-known mechanical phenomena which reflect the static viscoelasticity of materials. In the use of composite materials, the appearance of creep, stress relaxation and fatigue will directly affect the performance of composite materials [10-12]. In the actual working process of gaskets, the coupling effect of cyclic fatigue failure, creep and stress relaxation will occur under dynamic load. It will lead to the failure of gaskets and affect the working life of gaskets. The effects of creep and stress relaxation should be considered in the fatigue analysis of gaskets. It is necessary to investigate the influence of different fatigue cycles on the creep and stress relaxation behavior of materials, analyze the evolution mechanism of microstructure, and determine the damage mode.

Rubber matrix sealing composite material is a kind of typical viscoelastic materials, which has a common creep characteristics [13,14]. When the constant load is applied to the material, the deformation will gradually aggravate with the increase of time. If the load is large enough or duration is long enough, the internal micro damage will gradually accumulate in the material. Then the capacity of material to resist deformation decreases continuously, and the deformation rate accelerates until the specimen is broken completely. In the process of fatigue failure, micro-cracks and micro-holes will occur inside composite, which will inevitably influence the structure and mechanical properties of composites. As for creep damage of general composites, the performances are mainly affected by microstructures such as micro-cracks and micro-holes. Starting from these microscopic structures, the creep mechanism of materials are investigated by researchers [15-18]. With the development of mesomechanics

*Corresponding author: drzhbin@163.com

and micromechanics, the properties and responses of materials are not only just indivisible quantities on macro level, but also reflected in different multi-scale concepts from atom to micro to macro [19]. Xue *et al.* [20] studied the creep behavior of graphene-doped rubber. The damage mechanisms was investigated through observing the crack growth and fracture surface. The creep resistance of the rubber composites can be improved by graphene doping. The fiber/matrix interfacial properties played a major part in the creep behavior. Wang *et al.* [21] investigated the creep-recovery properties of polymer sealing composites. The Findley power law and the Weibull distribution function show good correspondence with the results of creep-recovery tests for composites. Sala *et al.* [22] investigated the effect of the stress level and environmental conditions on the creep recovery behavior of three kinds of composites. The fibers was made of flax, GreenPoxy and hemp, respectively. With the increase of stress level and the degradation of the environment, the levels of instantaneous, time-delayed and residual strains increased. The post-creep viscoelastic properties were determined by the anisotropic viscoelastic law on the basis of the recovery function. From the above, extensive studies about creep of composite material have been conducted. However, the creep behavior of rubber sealing composites materials after certain fatigue cycles is rarely studied, and it is worth further exploration.

In the bolted pipe flange connection system, stress relaxation is the major factor which leads to the decrease of bolt pretension and flange leakage failure. Stress relaxation is defined that the stress inside materials gradually attenuates with the increase of time under the condition of constant tensile deformation. When sealing gasket is installed on the connecting structure, stress relaxation will occur along with the increase of time. The fatigue phenomenon will happen when the material is subjected to fluctuating load, which will also have an impact on the properties and actual working life of the material. Therefore, it is very important to predict the stress relaxation after fatigue loading of such materials [23-25]. Related researches had been carried out on the stress relaxation behavior characteristics of composites. Mayencourt *et al.* [26] used mechanical spectroscopy to study interface stress-relaxation of composites. When the damping capacity was low, damage accumulation at the interface caused stress relaxation of the material. Mostafa [27] investigated the stress relaxation influence on fatigue cycles-to-failure of polymer composites. The results showed that residual stresses in the polymer matrix had fallen by 27 % within 110 days, and then the fatigue life dropped by 14 %. Some improvement measure was still feasible for long-term property optimization, though the stress relaxation within the polymer matrix reduced the improved fatigue cycles of composites. In conclusion, some studies of stress relaxation performance of composites have been conducted. However, the stress relaxation performance of fiber reinforced rubber

composites after different fatigue cycles is rarely reported.

Considerable work had already been accomplished on this research in our previous study, where the damage behavior and the fatigue properties of rubber matrix sealing composites were investigated [28,29]. This manuscript was a continuity of previous study to explore the creep and relaxation behavior of SFRC after different fatigue cycles. The creep and stress-relaxation curves were obtained. Then the microscopic defects were analyzed by SEM, and the damage patterns of SFRC were revealed. Finally, the parameters of new creep and stress relaxation models of SFRC after different fatigue cycles were determined.

Experimental

There were three main manufacturing processes of SFRC, namely, rubber mixing molding process, latex copying process and compression tensioning process. In addition, rubber mixing molding process was suitable for sample preparation in the laboratory. It required less production equipment, simple production process and small pollution. Therefore, the SFRC sample was prepared by rubber mixing molding in this research [28]. The component proportion of SFRC was shown in Table 1. The rubber and agents were purchased from Anhui Lixin Rubber Co. Aramid fiber Technora-T323SB (chopped fibers) was provided by Teijin-Twaron. The dumbbell-shaped specimens (Figure 1) cutting from the compression molded sheet were transverse direction. The whole length of specimen was 125 mm. The gauge length, width and gauge length are 25 mm, 6 mm and 2 mm, respectively. The experiment was conducted on the basis of Chinese standard [30]. Fatigue tests were carried out on a tensile testing machine (INSTRON 3367) under the cyclic pulsating load control. The stress amplitude was

Table 1. Component proportion of SFRC

Ingredients	Part per 100 rubber
NBR-3345	100
Aramid fiber	5.8
Sulphur	2
ZnO	2.5
Stearic acid	1
Accelerating agent	2
Anti-aging agent	2.5
Total	115.8

Table 2. General scheme of experiments

Test name	Fatigue number	Time (h)
Creep	0, 1000, 3000, 5000, 7000, 10000	20
Stress relaxation	0, 1000, 3000, 5000, 7000, 10000	20

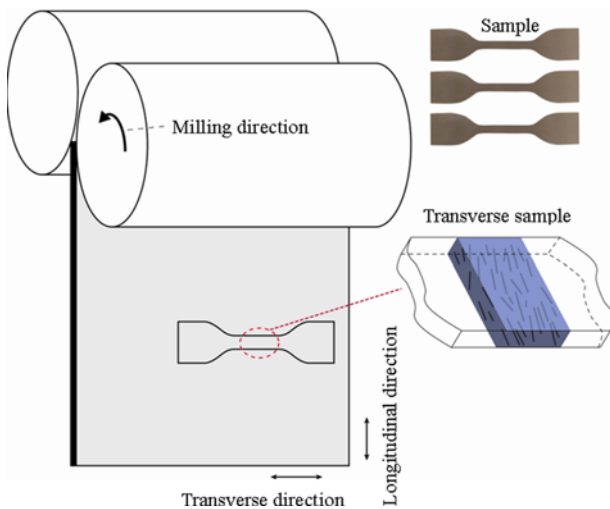


Figure 1. Sketches of the sample preparation.

assigned as 1 MPa at the stress ratio of 0. The tests were performed at a low frequency of 0.1 Hz to keep samples from overheating. The fractured surfaces of the SFRC were analyzed by the scanning electron microscope (JSM-5900). The test scheme was shown in Table 2. The experiment data was collected from three effective specimens.

Results and Discussion

Creep Characteristics after Fatigue Loading

The influence of fatigue cycles on the creep performance of SFRC was studied in the following conditions: 1) 5 % fiber mass fraction; 2) 1 MPa stress amplitude; 3) 0.1 Hz loading frequency; 4) 0 stress ratio. The creep load of 2 MPa was applied on the sample after fatigue loading. The curve of creep strain $\varepsilon(t)$ varying with time (t) of SFRC under different fatigue cycle (N_f) was shown in Figure 2. The creep strain increased with the increasing fatigue cycle as a whole. When the loading time reached 4 hours, the fatigue cycles

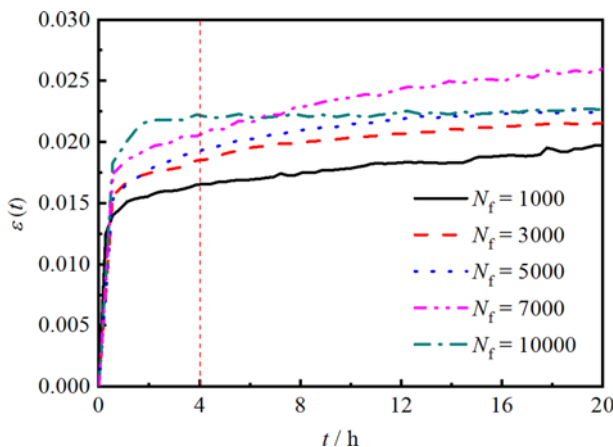


Figure 2. Creep curves of SFRC after different fatigue cycles.

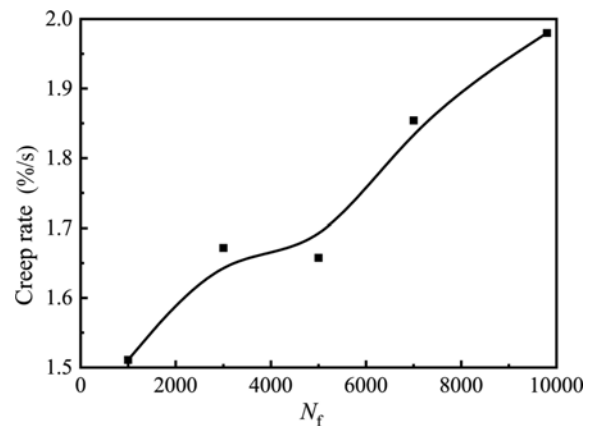


Figure 3. Initial creep rate of SFRC with different fatigue cycles.

(1000, 3000, 5000, 7000 and 10000) corresponded the creep strain of 0.0165, 0.0185, 0.0192, 0.0205, 0.0222, respectively. The creep curve of SFRC had obvious characteristics of the first two stages of the common creep curve. In the early period of creep (0-1 h), the creep rate was very fast. In the middle period of creep (1-20 h), the creep rate was slow and the creep variable remained basically unchanged. Figure 3 showed the curve of the creep rate with the creep time of 1 hour after different fatigue cycles. It can be found that the creep rate of SFRC materials increased nearly linearly with the increase of fatigue cycles.

SEM Analysis of Creep Specimen

Figure 4 and Figure 5 showed the SEM diagram of creep fracture of SFRC subjected to 1000 and 10000 fatigue cycles, respectively. Figure 4 showed that there were a large number of fracture fibers in the SFRC specimen section. In the rubber matrix, there were few holes caused by fiber/matrix interfacial debonding. The major damage mode of SFRC was fiber fracture. It can be seen from Figure 5 that there were a quantity of fracture fibers and a small number of holes in the section. The formation of holes in rubber matrix was mainly caused by the fiber/matrix interfacial

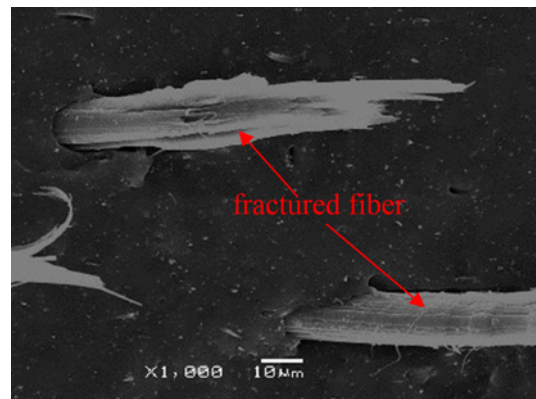


Figure 4. Creep fracture of SFRC after fatigue cycle of 1000.

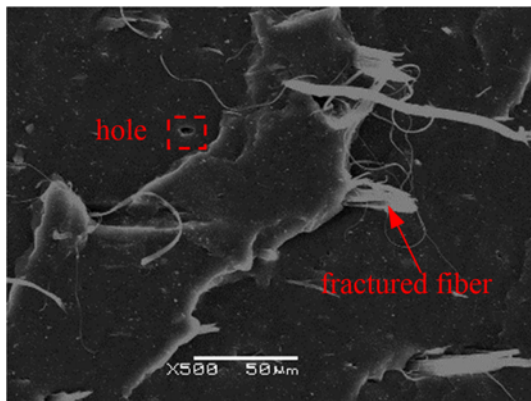


Figure 5. Creep fracture of SFRC after fatigue cycle of 10000.

debonding, which resulted in the fiber pulled out from the matrix. So fiber fracture and interfacial debonding were concomitant damage modes of SFRC in this condition. Above all, the fatigue cycles had considerable effect on the damage mode of creep sample.

Improved Creep Model

The elastoplastic creep constitutive model was proposed by Sakane [31], and the creep fatigue behavior of composites was investigated. The bilinear elastoplastic constitutive relation was used as the elastoplastic equation, and the following reinforcement properties of the material were considered. The creep constitutive equation of the material was as follows:

$$\varepsilon_c = A\sigma^B t \quad (1)$$

In the formula, A and B were regression coefficients. σ was the applied stress, MPa. ε_c was the creep strain. t was time, h.

The creep stress used in the test was 2 MPa, and the influence of fatigue cycles on creep performance was taken into consideration. Therefore, the equation (1) was modified, and the following equation (2) was obtained.

$$\varepsilon_c = (A_1 + A_2 \ln t)(A_3 + A_4 \log N_f) \quad (2)$$

In the formula, A_1 , A_2 , A_3 and A_4 were regression coefficients, which can be obtained by fitting the experimental data. N_f was fatigue cycle.

The creep strain calculation model based on equation (2) was modified, and the correlation coefficient in the formula was obtained through fitting analysis. The regression coefficient in equation (2) was obtained by fitting the results of creep test, and the results were shown in Table 3. The correlation coefficient obtained by improved model was 0.96, which was in good consistency with the experimental results. Taking SFRC subjected to 5000 fatigue cycles as an

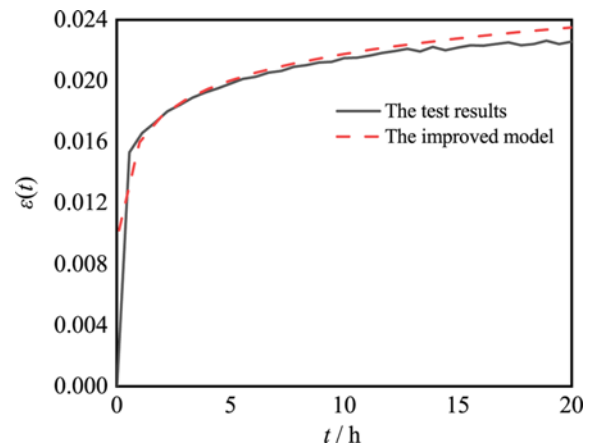


Figure 6. Comparison of creep test and the improved model.

Table 3. Regression coefficients of creep equation of SFRC

Regression coefficient	Coefficient values	Correlation coefficient
A_1	0.354	0.96
A_2	0.0556	
A_3	0.00593	
A_4	0.0106	

example, the data obtained from the test was compared with the improved creep strain model. The comparison results were shown in Figure 6. It can be found that the predicted results from the improved model were almost coincided with the experimental data. The results indicated that the improved model can efficiently characterize the creep performance of SFRC after fatigue.

Stress Relaxation Characteristics after Fatigue Loading

The influence of fatigue cycles on the stress relaxation performance of SFRC was studied. The load was applied on the sample until to 2 MPa, then the displacement was kept constant. The curve of stress $\sigma(t)$ with time (t) of SFRC were obtained, as shown in Figure 7. The results showed that SFRC had obvious relaxation properties. In the initial phase of stress relaxation, stress of SFRC rapidly attenuated with time. With the increase of time, the attenuation rate decreased gradually. When the time of stress relaxation attained 1 hour, the stress value of SFRC was reduced by 0.4-0.6 MPa after different fatigue cycles. When the time of stress relaxation reached 20 hours, the stress of SFRC dropped by 0.6-0.7 MPa. Therefore, the change of stress relaxation between 1 hour and 20 hours was not obvious, that is, the relaxation mainly occurred within the first hour.

It can be also found that the stress relaxation at low fatigue cycle was smaller than that at high fatigue cycle. The interface between fiber and matrix was well at low fatigue

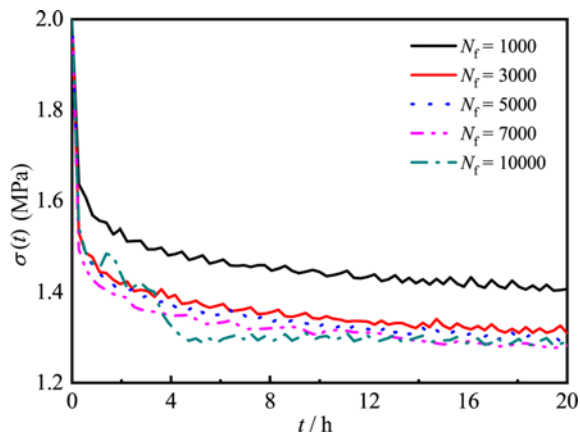


Figure 7. Relaxation curves of SFRC after different fatigue cycles.

cycles, which can effectively resist relaxation behavior. When the fatigue cycle was between 3000 and 7000, stress relaxation of SFRC did not change significantly. When the fatigue cycle was 10000, the stress relaxation curve of SFRC fluctuated greatly, which was caused by the alternation of various damage modes within SFRC (fiber fracture, matrix cracking and interfacial debonding).

SEM Analysis of Stress Relaxation Specimen

Figure 8 showed the surface morphology of stress relaxation of SFRC specimen after different fatigue cycles (1000, 3000, 7000 and 10000). It can be seen that the section morphology characteristics of stress relaxation specimens

after different fatigue cycles were similar to those of creep specimens. When the fatigue cycle was low, the interface between fiber and matrix was well bonded. With the increase of fatigue cycle, the interface between fiber and matrix began debonding, which eventually caused the fiber to be completely pulled out from the matrix.

Stress Relaxation Model

There were two main methods to study the stress relaxation model of composite materials. The first was based on the relaxation physical meaning of the material itself, and the corresponding physical model was established by means of mesomechanics and thermodynamics. The second was the phenomenological stress relaxation model. Its characteristic was to carry on the mathematics description to the stress relaxation test result, and it did not reflect the actual physical meaning of stress relaxation itself [27,32]. There were many models for the stress relaxation of isotropic polymers, but for rubber matrix composites after a certain fatigue cycle, the corresponding stress relaxation model had not been reported.

In this paper, stress relaxation curve of SFRC was characterized by a phenomenological stress relaxation model. The stress relaxation model of SFRC after fatigue can be expressed by the following equation:

$$\sigma(t) = \sigma_0 - (B_1 + B_2 \ln t)(B_3 + B_4 \log N_f) \tag{3}$$

In the formula, B_1 , B_2 , B_3 and B_4 were regression coefficients, which can be obtained by fitting the test data.

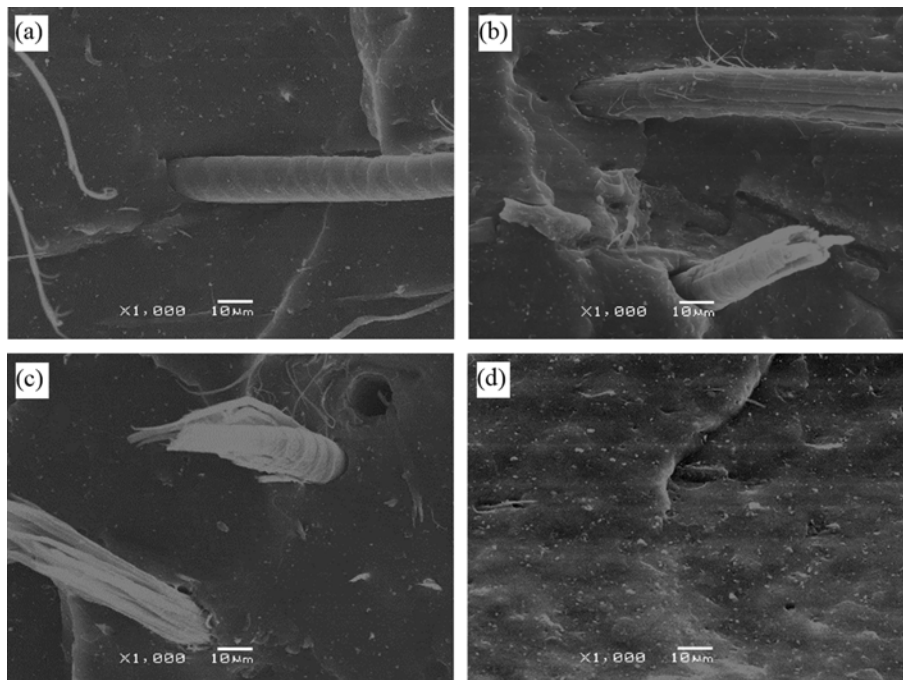


Figure 8. Relaxation fracture of SFRC after different fatigue cycles; (a) $N_f=1000$, (b) $N_f=3000$, (c) $N_f=7000$, and (d) $N_f=10000$.

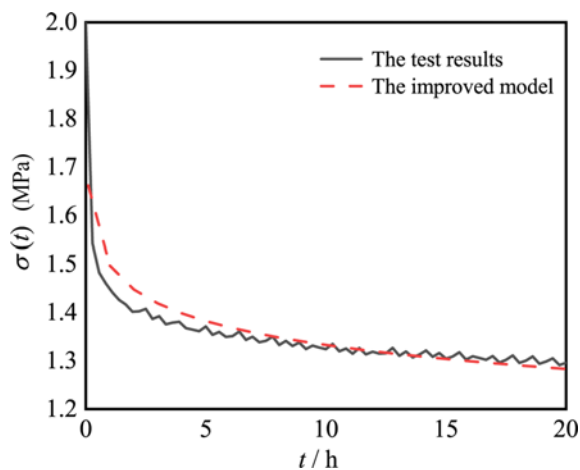


Figure 9. Comparison of stress relaxation test and the improved model.

Table 4. Regression coefficients of stress relaxation equation of SFRC

Regression coefficient	Coefficient values	Correlation coefficient
B_1	0.359	0.95
B_2	0.0510	
B_3	0.324	
B_4	0.291	

The correlation coefficient in the formula was obtained through fitting analysis. The above regression coefficients were obtained by fitting the stress relaxation curve measured in the test, and the results were listed in Table 4. The correlation coefficient obtained by improved model was 0.95, which was in good consistency with the experimental results. When SFRC was subjected to 5000 fatigue times, the data obtained from the test were compared with the improved stress relaxation model. The comparison consequences were shown in Figure 9. The results declared that the improved stress relaxation calculation model was in good consistency with the experimental results. It can well characterize the relaxation behavior of SFRC after fatigue cycle.

Conclusion

In this paper, the creep and relaxation behaviors of SFRC after different fatigue cycles were obtained by experiment. The main research contents and results were as follows.

The creep strain curves of SFRC after certain fatigue cycles were obtained. The test results indicated that the creep strain aggravated as the fatigue cycles increased. SEM analysis verified that the fatigue cycles had remarkable

influence on the damage mode of SFRC after creep. The creep damage modes changed from the fiber fracture to interfacial debonding with the increase of the fatigue cycles. The modified creep model can well characterize the creep properties of SFRC material with different fatigue cycle.

The stress relaxation curves of SFRC after certain fatigue cycles were also obtained. The test results revealed that SFRC had obvious relaxation characteristics and its stress relaxation mainly occurred in the first hour, which meant that the bolted flange connection system should be loaded again after one hour. The stress relaxation model of SFRC after different fatigue cycles was established, and the predicting results were consistent with test results.

Acknowledgements

This project is supported by National Natural Science Foundation of China (Grant No. 51705037), by Scientific Research Foundation for Advanced Talents (Grant No. XZ1633), by Natural Science Foundation of the Jiangsu Higher Education Institutions of China (Grant No. 19KJB130002), by the “Six Talent Peaks” high-level talent projects (Grant No. GDZB-061, GDZB-063).

References

1. B. Zhang, X. Yu, and B. Gu, *Fiber. Polym.*, **18**, 349 (2017).
2. X. Yu, B. Gu, and B. Zhang, *Fiber. Polym.*, **16**, 2258 (2015).
3. L. Chen and B. Gu, *Polym. Compos.*, **39**, 1455 (2018).
4. B. Zhang, X. Yu, and B. Gu, *Polym. Compos.*, **38**, 381 (2017).
5. N. Korneeva, V. Kudinov, I. Krylov, and V. Mamonov, *Polym. Eng. Sci.*, **57**, 693 (2017).
6. M. Rafiqzaman, S. Abdullah, and A. M. T. Arifin, *Fiber. Polym.*, **16**, 640 (2015).
7. J. H. Yan, K. Liu, H. Zhou, Z. W. Zhang, B. H. Gu, and B. Z. Sun, *Fiber. Polym.*, **16**, 634 (2015).
8. I. E. Sawi, Z. Fawaz, R. Zitoune, and H. Bougherara, *J. Mater. Sci.*, **49**, 2338 (2014).
9. S. C. Garcea, I. Sinclair, and S. M. Spearing, *Compos. Sci. Technol.*, **109**, 32 (2015).
10. J. H. Almeida, H. L. Ornaghi, N. Lorandi, G. Marinucci, and S. Amico, *Polym. Eng. Sci.*, **58**, 1837 (2018).
11. A. Kühn and P. A. Muñoz-Rojas, *Mech. Adv. Mater. Struct.*, **1** (2019).
12. Z. Jiang, P. Liu, H. J. Sue, and T. Bremner, *Polymer*, **160**, 231 (2019).
13. F. Daver, M. Kajtaz, M. Brandt, and R. A. Shanks, *Polymers*, **8**, 437 (2016).
14. M. Eftekhari and A. Fatemi, *Fatigue Fract. Eng. M.*, **38**, 1395 (2015).
15. N. V. David, X. L. Gao, and J. Q. Zheng, *Mech. Adv. Mater. Struct.*, **20**, 464 (2013).

16. L. H. Wang, *Compos. Sci. Technol.*, **130**, 1 (2016).
17. Y. Cui, J. E. Campbell, M. Burley, M. Patel, K. Hunt, and T. W. Clyne, *Mech. Mater.*, **148**, 103461 (2020).
18. X. Liu, S. Zhang, X. J. Xu, Z. Zhang, L. Zhou, and G. Zhang, *Fiber. Polym.*, **14**, 1635 (2013).
19. S. Ravindran, N. Mani, S. Balaji, M. Abhijith, and K. Surendaran, *Mater. Today: Proceedings*, **16**, 1020 (2019).
20. C. Xue, H. Y. Gao, Y. C. Hu, and G. X. Hu, *Polym. Test.*, **87**, 106509 (2020).
21. Z. Wang, S. Shen, A. Zhou, and H. Lyu, *J. Appl. Polym. Sci.*, **138**, e49946 (2020).
22. B. Sala, X. Gabrion, F. Trivaudey, V. Guicheret-Retel, and V. Placet, *Compos. Part A-Appl. S.*, **141**, 106204 (2021).
23. D. F. Zhao, Y. Y. Dong, J. Xu, Y. Q. Yang, K. Fujiwara, E. Suzuki, T. Furukawa, Y. Takai, and H. Hamada, *Fiber. Polym.*, **17**, 2131 (2016).
24. C. Brosseau, A. Mdarhri, and A. Vidal, *J. Appl. Phys.*, **104**, 074105 (2008).
25. H. M. Brodowsky, W. Jenschke, and E. Mäder, *Compos. Part A-Appl. S.*, **41**, 1579 (2010).
26. C. Mayencourt and R. Schaller, *Mat. Sci. Eng. A.*, **325**, 286 (2002).
27. N. H. Mostafa, *Mech. Time-Depend. Mat.*, **23**, 497 (2019).
28. B. Zhang, X. Yu, and B. Gu, *Polym. Eng. Sci.*, **58**, 920 (2018).
29. B. Zhang, B. Gu, and X. Yu, *J. Appl. Polym. Sci.*, **132**, 41672 (2015).
30. GB/T 1688: 2008, Rubber, vulcanized-Determination of Tension Fatigue, 2018.
31. M. Sakane, M. Ohnami, T. Awaya, and N. Shirafuji, *J. Eng. Mater. Technol.*, **111**, 54 (1989).
32. V. Djoković and J. M. Nedeljković, *Macromol. Rapid Comm.*, **21**, 994 (2000).